

## Right Fusiform and Right Angular Gyrus Activity as the Source to Famous and Unfamiliar Faces Response.

Eline Poinsignon-Clavel

	P100		N135	
	Amplitude (fT)	Latency (ms)	Amplitude (fT)	Latency (ms)
<b>Famous face</b>	253.7	88	-132.4	162
<b>Unfamiliar face</b>	207.2	87	-145.6	159
<b>Scrambled</b>	223.2	89	-128.3	145

**Table 1 – Amplitude and latency of the visually-evoked response field at P100 and N135 after visual stimuli of famous, unfamiliar, and scrambled faces.** This table shows data taken from Wakeman & Henson’s 2015 study<sup>1</sup> and was measured on Brainstorm<sup>2</sup>. The data represents MEG recordings from the right parieto-occipital sensor (MEG2322) of a young healthy adult male with 20/20 visual acuity. The subject was presented with a series consisting of each of the 3 face types (150 stimuli over 7.5mins, 50 stimuli of each face type) where each stimulus was presented for 800-1000ms. Each stimulus was separated by an interstimulus interval (a white circle) for 1700ms. 306 channel MEG was used with 3 surface fiducial points (matched with MRI for figure 1). The acquisition rate was 1100Hz. Low pass = 32Hz, high pass = 1Hz, notch = 50Hz.

For P100, there was no difference in amplitude between the face conditions and the non-face condition (scrambled); scrambled amplitude (223.2 fT) was between the amplitudes of the 2 face conditions (207.2 fT and 253.7 fT ). Scrambled latency (89ms) was slightly longer than the face conditions (87ms and 88ms) but extremely similar to the famous face condition (88ms). Overall, each condition had very similar P100 latencies.

For N135, amplitude of the scrambled condition was smaller (-128.3 fT) than the face conditions (-132.4 fT and -145.6 fT), though the difference in amplitude remains bigger between famous and unfamiliar faces (-13.2 fT) than between scrambled and famous faces (-4.1 fT). N135 latency was significantly shorter for the scrambled condition (145ms) than the face conditions (159ms and 162ms).

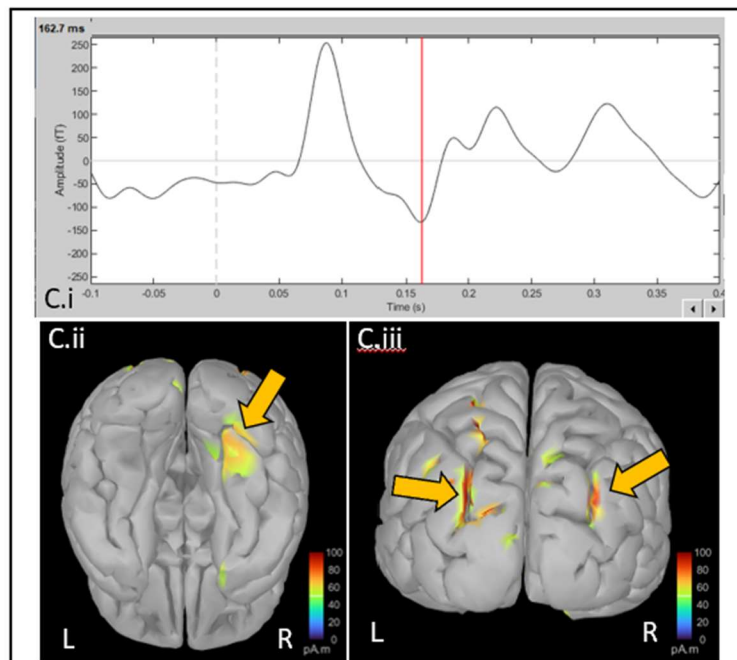
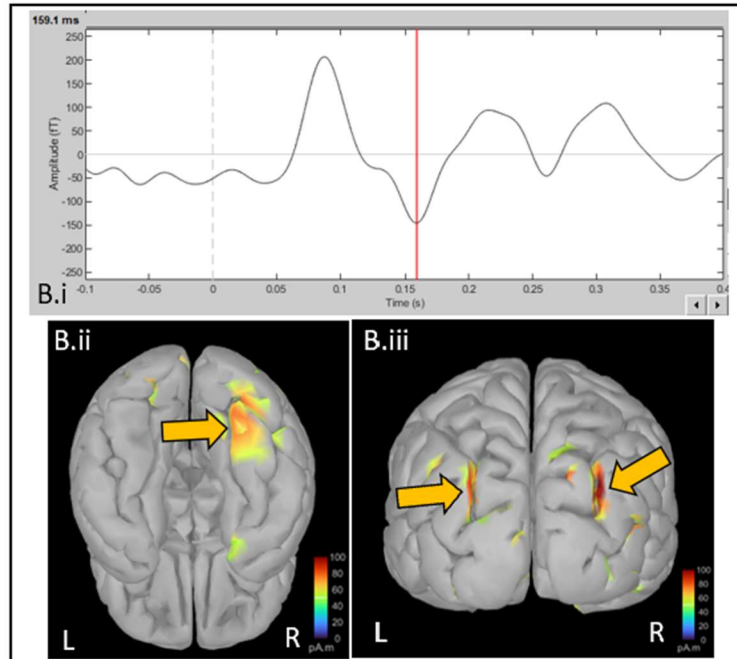
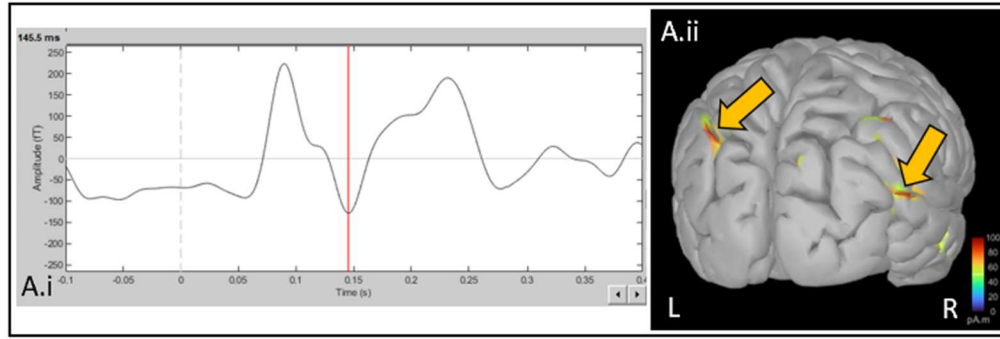


**Figure 1 – Source localization and waveform of visually evoked response field from scrambled, unfamiliar, and famous face stimuli at N135.** These images were produced using Brainstorm<sup>2</sup> by correcting for noise again and creating a 3D head model of the patient based on his T1 MRI scans (Siemens 3T) which was previously standardized to MNI152. MEG magnetometers were removed for noise correction, only MEG gradiometers were selected for these images. A scale of 0-100pAm is used to measure standardized activity across MRI/MEG images.

Figure 1.A.i) Response to scrambled stimuli at 145ms along the MEG waveform. 1.A.ii) Image is in coronal view (slightly moved to the left for better visualization of ROIs), looking at the occipital lobe. Yellow arrows point to the source of the visual stimuli response in the left (MNI was  $x=-31.4$ ,  $y=-73.1$ ,  $z=51.8$ ) and right inferior parietal lobe (MNI was  $x=57.5$ ,  $y=-59.9$ ,  $z=19.2$ ). Power in the left inferior parietal lobe was  $8.1962e-11$ , and right inferior parietal lobe was  $8.9768e-11$ .

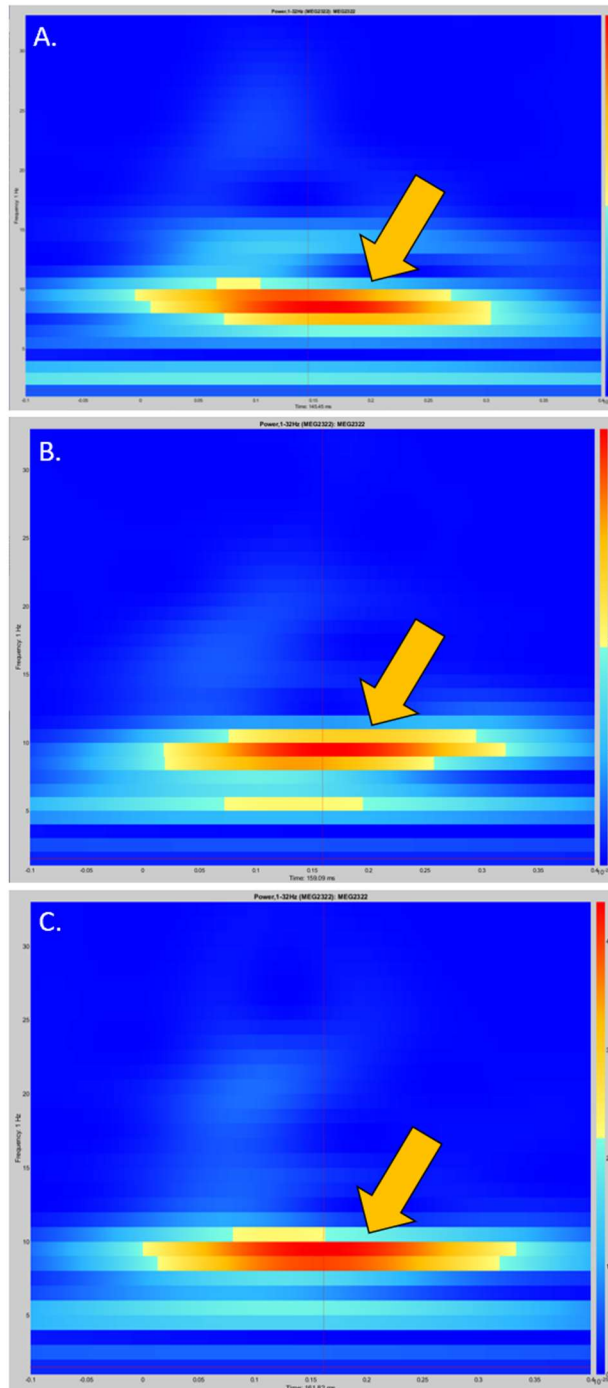
Figure 1.B.i) Response to unfamiliar face stimuli at 159ms along the MEG waveform. 1.B.ii) Image is in ventral view. Yellow arrows point to the source of the visual stimuli response in the right fusiform (MNI was  $x=31.1$ ,  $y=-66.1$ ,  $z=-18.2$ ). Power in the right fusiform was  $7.6286e-11$ . 1.B.iii) Image is in coronal view, looking at the occipital lobe. Yellow arrows point to the source of the visual stimuli response in the left (MNI was  $x=-27.0$ ,  $y=-83.3$ ,  $z=34.7$ ) and right inferior parietal lobe (MNI was  $x=34.3$ ,  $y=-81.8$ ,  $z=37.3$ ). Power in the left inferior parietal lobe was  $8.2208e-11$ , and right inferior parietal lobe was  $1.064e-10$ .

Figure 1.C.i) Response to famous face stimuli at 162ms along the MEG waveform. 1.C.ii) Image is in ventral view. Yellow arrows point to the source of the visual stimuli response in the right fusiform (MNI was  $x=31.1$ ,  $y=-66.1$ ,  $z=-18.2$ ). Power in the right fusiform was  $6.7112e-11$ . 1.C.iii) Image is in coronal view, looking at the occipital lobe. Yellow arrows point to the source of the visual stimuli response in the left (MNI was  $x=-27.0$ ,  $y=-83.3$ ,  $z=34.7$ ) and right inferior parietal lobe. Right inferior parietal lobe MNI and power was not recorded. Power in the left inferior parietal lobe was  $9.6649e-11$ .

In the scrambled condition, the precise location of the activity in the left inferior parietal lobe was the left visual motor, and the right inferior cortex activity location was the right angular gyrus<sup>3</sup>. The right angular gyrus was slightly more active ( $8.9768e-11$ ) than the left visual motor ( $8.1962e-11$ ).

In the unfamiliar face condition, the activity in the left and right inferior parietal lobe was precisely in the left and right angular gyrus<sup>3</sup>. The right angular gyrus was a lot more active ( $1.064e-10$ ) than the left angular gyrus ( $8.2208e-11$ ), and the right fusiform was the least active ( $7.6286e-11$ ).

In the famous face condition, the left inferior parietal lobe activity was also situated in the left angular gyrus<sup>3</sup>. The activity was higher in the left angular gyrus ( $9.6649e-11$ ) than in the right fusiform ( $6.7112e-11$ ). The right inferior parietal lobe cannot be compared due to lack of data. Overall, the right angular gyrus was the most active region across the different conditions, its most active state being in the unfamiliar face condition. The right fusiform was more active in the unfamiliar face condition than in the familiar face condition.



**Figure 2 – Highest activity recorded around 9-10Hz across all 3 face conditions in time-frequency response plots.** These time-frequency response (TFR) plots were created using Brainstorm<sup>2</sup>. They show the frequencies driving the N135 visually evoked field responses to the different face stimuli from the MEG2322 sensor. X-axis is latency (ms), y-axis is frequency (Hz), colours are amplitude (fT) (legend on the right of each image).

A) Scrambled condition TFR plot. Crosshair indicates time of N135 response at 145ms. The yellow arrow points to the highest amplitude (red) which was mostly at a frequency of 9Hz. The band right above 9Hz was a slightly less bright red at 10Hz.

B) Unfamiliar face condition TFR plot. Crosshair indicates time of N135 response at 159ms. The yellow arrow points to the highest amplitude (red) which was at a frequency of 10Hz.

C) Famous face condition TFR plot. Crosshair indicates time of N135 response at 162ms. The yellow arrow points to the highest amplitude (red) which was at a frequency of 10Hz. The band right below was a slightly less bright red at 9Hz.

The scrambled condition's most active frequency was 9Hz while the unfamiliar and famous face conditions' most active frequency was 10Hz. However, the unfamiliar face condition was the only one with a singular red band (highest activity) at 10Hz, the other 2 conditions had a secondary red band which accounted for a little less activity than the

major band, but were still significant as they were still demonstrating very high activity. Overall, all 3 conditions exhibited most activity at very similar frequencies, though the scrambled condition showed most activity at a slightly lower frequency than the 2 face conditions.

## Discussion

The scrambled condition showed a shorter N135 latency and amplitude than the 2 face conditions as mentioned in Table 1. Rossion & Caharel's 2011 study found that the N135 amplitude was larger in intact visual stimuli (such as faces) than in scrambled stimuli, and N135 latency was shorter in scrambled stimuli than for intact visual stimuli. They explained this phenomenon with the contribution of object shape-sensitive visual processes in areas like the lateral occipital complex or more importantly, the right fusiform, in the N135 response. Scrambled stimuli do not have to be processed by such brain areas and therefore do not elicit N135 amplitudes as high as intact stimuli<sup>4</sup>. The activity observed in the right fusiform was only in seen in the 2 face conditions as it consists of the fusiform face area. This is an area specialized in face perception and discrimination between familiar and unfamiliar faces<sup>5,6</sup>. The higher activity level found in the right fusiform for unfamiliar faces compared to familiar faces opposes Weibert & Andrews's 2015 study which showed a higher response in the right fusiform for familiar face compared to unfamiliar<sup>7</sup>. This is likely due to the reduced right fusiform response associated with repeated exposure of familiar faces and the increased activity associated with repeated exposure of unfamiliar faces, which was the case in the experiment our data came from<sup>6</sup>. The activity recorded in the right angular gyrus across all 3 conditions may be due to its major role played in the semantic system required in perception and identification of visual input, hence facial recognition<sup>8</sup>. One of its main processes is also responsible for memory retrieval<sup>9</sup>. This would explain why the highest level of activity observed in the right angular gyrus was in the unfamiliar face condition as this is the condition where it would need to work more to make sure the face is unfamiliar.

Schizophrenia is characterized by auditory and visual hallucinations, as well as impaired social skills. This disorder alters facial and emotional expression processing, and patients' deficits in emotional processing are predictive of clinical outcome<sup>10</sup>. Shah et al.'s 2018 study on schizophrenic patients' impaired emotional face processing aimed to look at whether the impairments came from early visual and face processing or from later high-order cognitive function. They also wanted to know whether the impairments were specific to neutral, emotional, or very specific emotional expressions. The study used 32 EEG electrodes placed in accordance to the 10-10 system of electrode placement. More electrodes were placed on the external canthi and orbital ridges of patients' eyes to minimize noise from eye movements, and on the mastoids to act as references along with a frontally positioned electrode. EEG activity was sampled at 500Hz and the filters applied were set to 0.1-30.0Hz. They presented patients with 20 faces, each expressing one of five emotional expression (sadness, fear, joy, anger, neutral), along with 4 images of a chair. After each image, patients had to identify the emotion expressed. Each participant went through 408 trials. The findings stated that schizophrenic patients had a lower P100 amplitude than controls when exposed to fearful, sad, and angry facial expressions as well as the chair stimuli. N170 amplitude was smaller for patients with schizophrenia in joyful, neutral, fearful, and angry expressions, as well as chair stimuli. Lastly, P300 mean activity was smaller in schizophrenic patients across all facial expressions and chair stimuli. Overall, they found different amplitude patterns for P100 and N170 in patients than the ones found in controls. The findings related to their study objectives demonstrated that impairments are equally seen across all 5 emotional expressions and not specifically to negative expressions. They also mentioned that deficits begin in early sensory processing and proceed to higher-order processing deficits. Visually evoked responses (VER) can therefore be useful as a diagnostic tool for

schizophrenia. We can identify the disorder based on the typical changes observed in patients VERs such as lower amplitudes for certain emotions at different time points (P100, N170, P300) as found in Shah et al.'s 2018 study.

## References

1. Wakeman DG, Henson RN, A multi-subject, multi-modal human neuroimaging dataset, Scientific Data (2015).
2. Tadel F, Baillet S, Mosher JC, Pantazis D, Leahy RM. Brainstorm: A User-Friendly Application for MEG/EEG Analysis. *Comp Intel Neurosci.* 2011:879716.
3. BioImage Suite MNITAL. bioimagesuitewebgithubio.  
<https://bioimagesuiteweb.github.io/webapp/mni2tal.html>
4. Rossion, B., & Caharel, S. (2011). ERP evidence for the speed of face categorization in the human brain: Disentangling the contribution of low-level visual cues from face perception. *Vision Research*, 51(12), 1297–1311. <https://doi.org/10.1016/j.visres.2011.04.003>
5. Kanwisher, N., McDermott, J., & Chun, M. M. (1997). The Fusiform Face Area: A Module in Human Extrastriate Cortex Specialized for Face Perception. *The Journal of Neuroscience*, 17(11), 4302–4311. <https://doi.org/10.1523/jneurosci.17-11-04302.1997>
6. Rossion, B., Schiltz, C., & Crommelinck, M. (2003). The functionally defined right occipital and fusiform “face areas” discriminate novel from visually familiar faces. *NeuroImage*, 19(3), 877–883. [https://doi.org/10.1016/s1053-8119\(03\)00105-8](https://doi.org/10.1016/s1053-8119(03)00105-8)
7. Weibert, K., & Andrews, T. J. (2015). Activity in the right fusiform face area predicts the behavioural advantage for the perception of familiar faces. *Neuropsychologia*, 75, 588–596. <https://doi.org/10.1016/j.neuropsychologia.2015.07.015>
8. Seghier, M. L., Fagan, E., & Price, C. J. (2010). Functional Subdivisions in the Left Angular Gyrus Where the Semantic System Meets and Diverges from the Default Network. *Journal of Neuroscience*, 30(50), 16809–16817. <https://doi.org/10.1523/jneurosci.3377-10.2010>
9. Seghier, M. L. (2012). The Angular Gyrus. *The Neuroscientist*, 19(1), 43–61. <https://doi.org/10.1177/1073858412440596>
10. Shah, D., Knott, V., Baddeley, A., Bowers, H., Wright, N., Labelle, A., Smith, D., & Collin, C. (2018). Impairments of emotional face processing in schizophrenia patients: Evidence from P100, N170 and P300 ERP components in a sample of auditory hallucinators. *International Journal of Psychophysiology*, 134, 120–134. <https://doi.org/10.1016/j.ijpsycho.2018.10.001>